A New Optical Flow Estimation Method In Joint EO/IR Video Surveillance

Hong Man[1], Robert J. Holt[2], Jing Wang[1], Rainer Martini[1], Ravi Netravali[1], Iraban Mukherjee[1]

[1] Center for Intelligent Networked Systems, Stevens Institute of Technology Hoboken, NJ 07030

[2] Dept. of Mathematics and Computer Science, City University of New York, Bayside, NY 11364

ABSTRACT

Electro-Optical (EO) and Infra-Red (IR) sensors have been jointly deployed in many surveillance systems. In this work we study the special characteristics of optical flow in IR imagery, and introduce an optical flow estimation method using co-registered EO and IR image frames. The basic optical flow calculation is based on the combined local and global (CLG) method (Bruhn, Weickert and Schnorr, 2002), which seeks solutions that simultaneously satisfy a local averaged brightness constancy constraint and a global flow smoothness constraint. While CLG method can be directly applied to IR image frames, the estimated optical flow fields usually manifest high level of random motions caused by thermal noise. Furthermore, IR sensors operating at different wavelengths, e.g. meddle-wave infrared (MWIR) and long-wave infrared (LWIR), may yield inconsistent motions in optical flow estimation. Because of the availability of both EO and IR sensors in many practical scenarios, we propose to estimate optical flow jointly using both EO and IR image frames. This method is able to take advantage of the complementary information offered by these two imaging modalities. The joint optical flow calculation fuses the motion fields from EO and IR images using a cross-regularization mechanism and a non-linear flow fusion model which aligns the estimated motions based on neighbor activities. Experiments performed on the OTCBVS dataset demonstrated that the proposed approach can effectively eliminate many unimportant motions, and significantly reduce erroneous motions, such as sensor noise.

Keywords: optical flow, infrared imaging, multimodal imagery, visual surveillance, multi-sensor fusion

1. INTRODUCTION

Many existing surveillance systems are now equipped with both visible light electro-optical (EO) cameras and infrared (IR) cameras. However most of these cameras are operated separately, with EO cameras mainly producing day-light visions, and IR cameras producing night visions. Intuitively we recognize that EO and IR cameras may provide complementary information if they are used jointly. An EO image mostly represents the intensities of reflected visible lights from certain object in the field of view, while an IR image captures the thermal profile of the object. The objective of this work is to study effective methods that can fuse the visual information from these two types of cameras for motion analysis in the context of surveillance and monitoring.

IR images are normally of low resolution and are lack of distinctive textures. However, it can easily highlight heated objects regardless of light conditions. IR images are formed on the basis of heat emissivity, conductivity as well as reflection properties of material surface. On the other hand, EO images provide better color, texture, and shape features of the target object. But they are very sensitive to illumination variations, which may be caused by weather, shadow, time of day, and/or multiple light sources etc. Therefore, joint EO/IR systems have become attractive solutions for providing robust detection and tracking performance under various practical operation environments. In[1],[2] Kang et al. introduced an interesting example of joint EO/IR system for surveillance, in

Further author information:
E-mail: {jwang, hman, rmartini, imukherj}@stevens.edu, ran2290@gmail.com, rjh@research.bell-labs.com
Corresponding author: Hong Man

Infrared Imaging Systems: Design, Analysis, Modeling, and Testing XVIII,
edited by Gerald C. Holst, Proc. of SPIE Vol. 6543, 65430P, (2007)
0277-786X/07/$18 · doi: 10.1117/12.719164

which a joint probability model for EO and IR features was proposed for data fusion, and a Kalman filter was used to track objects and resolve occlusions.

Motion estimation is an important component in computer vision and video analysis. The 3D motion of a scene can be described by a motion field, which specifies the 3D velocities at each point of the scene. In a captured 2D image, the 3D motion field is only represented by its 2D projection, which can be estimated in the form of "optical flow". Optical flow is a velocity field in the image which transforms one image into the next image in a sequence.[3] The velocities in optical flow represent the spatial variations of pixel brightness or color intensity in the image.

Optical flow estimation has been extensively studied since 1980's. Existing methods are mostly based on computing the spatial and temporal image derivatives, which are referred to as "differential methods". Depending on the optimization criteria, most methods can be classified into two generally categories.[4] The criteria of the first category are based on local constancy constraints, and the criteria of the second category include certain global flow energy measures. Example works belonging to the first category include Lucas and Canade (1981),[5] Lucas (1984),[6] Bigün and Granlund (1988),[7] Golland and Bruckstein (1997)[8]; and works belonging to the second category include Horn and Schunck (1981),[3] Nagel and Enkelman (1983),[9] Bruhn et al. (2002),[10] Brox et al. (2004).[11] Two benchmark studied were reported by Barron et al. (1994)[12] and Galvin et al. (1998) —citegalvin98, which concluded that local methods may have higher robustness to noise, but can not produce dense flow field, and global methods can produce dense flow filed but are sensitive to noise. While most of the optical flow works are based on visible light images, Haussecker and Fleet (2001)[13] studied optical flow estimation on infrared images where brightness constancy may be violated. To the best of authors' knowledge, no work have been done on optical flow estimation on joint EO and IR images.

The rest of this paper is organized as follows. In Section 2 we introduce the basic optical flow theory and two estimation methods. In Section 3 we introduce present detailed discussion on the methods for joint EO/IR optical flow estimation. The experimental results are provided in Section 4. The paper is concluded in Section 5.

2. OPTICAL FLOW

A fundamental assumption in optical flow estimation is "brightness constancy", which states that the brightness of each point of the object in the image is invariant under motion. Given an object point P, at time t, its position in the image is $\mathbf{x} = [x, y]^t$, and its 2D projection of velocity vector in the image is $\mathbf{u} = [u, v]^t$. After a time δt, the new position of this point becomes $\mathbf{x} + \mathbf{u}\delta t = [x + u\delta t, y + v\delta t]^t$. Let the brightness of this point at time t be $I(\mathbf{x}, t)$, the brightness constancy assumption can be expressed as

$$I(\mathbf{x}, t) = I(\mathbf{x} + \mathbf{u}\delta t, t + \delta t). \tag{1}$$

$$u(x, y, t) = \frac{dx}{dt}, \quad v(x, y, t) = \frac{dy}{dt} \tag{2}$$

are the components of optical flow vector at $P(x, y, t)$. Equation (1) can be expanded in Taylor series as

$$I(\mathbf{x}, t) = I(\mathbf{x}, t) + \frac{\partial I}{\partial x}u\delta t + \frac{\partial I}{\partial y}v\delta t + \frac{\partial I}{\partial t}\delta t + O(\delta t^2). \tag{3}$$

Assuming small displacements and delay, we have

$$\frac{\partial I}{\partial x}u + \frac{\partial I}{\partial y}v + \frac{\partial I}{\partial t} = 0, \tag{4}$$

which is the main optical flow constraint equation. $\frac{\partial I}{\partial x}$, $\frac{\partial I}{\partial y}$ and $\frac{\partial I}{\partial t}$ are quantities observed from the image sequence, and $[u, v]^t$ are to be calculated. Apparently equation (4) alone is not sufficient to determine the two unknowns in $[u, v]^t$, which is known as the "aperture problem"[14] , additional constraints are needed.

2.1. Motion from Color Method

Among various constraints been proposed over the years, one approach appears to have direct relevance to joint EO and IR video analysis, that is optical flow from color images. Ohta[15] and Golland and Bruckstein[8] studied multiple constraints based on functions that are extracted from R, G and B color channels. Similar to brightness constancy assumption, this approach assumes invariance of three color components. More specifically this assumption implies that the (R, G, B) or (H, S, I) values of a certain point in the image will not change under motion of this point. This provides three separate constraints.[8]

$$\frac{\partial I_R}{\partial x}u + \frac{\partial I_R}{\partial y}v + \frac{\partial I_R}{\partial t} = 0, \tag{5}$$

$$\frac{\partial I_G}{\partial x}u + \frac{\partial I_G}{\partial y}v + \frac{\partial I_G}{\partial t} = 0, \tag{6}$$

$$\frac{\partial I_B}{\partial x}u + \frac{\partial I_B}{\partial y}v + \frac{\partial I_B}{\partial t} = 0. \tag{7}$$

The solution to these equations can be expressed as

$$\mathbf{u} = (A^t A)^{-1} A^t b, \tag{8}$$

where

$$A = \begin{bmatrix} I_{Rx} & I_{Ry} \\ I_{Gx} & I_{Gy} \\ I_{Bx} & I_{By} \end{bmatrix}, b = \begin{bmatrix} -I_{Rt} \\ -I_{Gt} \\ -I_{Bt} \end{bmatrix}. \tag{9}$$

The necessary condition of this solution is that $A^t A$ is not singular. However this condition may easily be violated because correlations frequently exist among RGB components in nature images. In such cases, Golland and Bruckstein[8] used the condition number of matrix $A^t A$ to indicate the confidence of the pseudo-inverse solution.

2.2. Combined Local and Global Optical Flow Method

The pioneering works by Lucas and Kanade (1981)[5] and Horn and Schunch (1981)[3] remain to be highly influential in optical flow field. The Lucas-Kanade method is focused on local flow constraint and the Horn-Schunch method emphasizes global flow coherence. One of the major progress in recently years is the combined local and global (CLG) optical flow method by Bruhn, Weickert and Schnorr (2002)[10] , which essentially incorporates the Lucas-Kanade method with the Horn-Schunch method. This approach appears to be very successful. In this section we review the basic formulations of these methods.

Equation (4) describes the original intensity constancy constraint, which can be re-written as

$$E = \begin{bmatrix} I_x & I_y & I_t \end{bmatrix} \begin{bmatrix} u \\ v \\ 1 \end{bmatrix} = 0. \tag{10}$$

Because this constraint is not enough for solving $[u, v]^t$, the Lucas-Kanade method employs a squared constraint

$$E^2 = \begin{bmatrix} u & v & 1 \end{bmatrix} \begin{bmatrix} I_x \\ I_y \\ I_t \end{bmatrix} \begin{bmatrix} I_x & I_y & I_t \end{bmatrix} \begin{bmatrix} u \\ v \\ 1 \end{bmatrix} = \begin{bmatrix} u & v & 1 \end{bmatrix} \mathbf{J} \begin{bmatrix} u \\ v \\ 1 \end{bmatrix}, \tag{11}$$

where

$$\mathbf{J} = \begin{bmatrix} I_x^2 & I_x I_y & I_x I_t \\ I_y I_x & I_y^2 & I_y I_t \\ I_t I_x & I_t I_y & I_t^2 \end{bmatrix} \tag{12}$$

which is called "motion tensor". To introduce certain robustness to local noise, Lucas and Kanade defined a modified energy function

$$E_{LK} = \begin{bmatrix} u & v & 1 \end{bmatrix} (G_\rho * \mathbf{J}) \begin{bmatrix} u \\ v \\ 1 \end{bmatrix}, \tag{13}$$

where G_ρ is a local smooth mask, usually a Gaussian. The Lucas-Kanade method seeks solution $[u, v]^t$ to minimize E_{LK}, which leads to the linear equation

$$G_\rho * \begin{bmatrix} I_x^2 & I_x I_y & I_x I_t \\ I_y I_x & I_y^2 & I_y I_t \end{bmatrix} \begin{bmatrix} u \\ v \\ 1 \end{bmatrix} = 0. \tag{14}$$

Because the system matrix of these linear equations may be singular, especially in flat regions, the Lucas-Kanade method usually has difficult to produce dense flow fields.

In order to achieve dense flow estimation, the Horn-Schunck method embeds local optical flow constraint in a global regularization framework. A global energy function is defined as

$$E_{HS} = \int_\Omega (\begin{bmatrix} u & v & 1 \end{bmatrix} \mathbf{J} \begin{bmatrix} u \\ v \\ 1 \end{bmatrix} + \alpha(|\nabla u|^2 + |\nabla v|^2)) dxdy \tag{15}$$

where $\nabla f = [f_x, f_y]^t$, and α is the regularizing parameter. Larger α leads to smoother flow fields and vice versa. The Horn-Schunck method seeks solution $[u, v]^t$ that minimize E_{HS}. It can be observed that, in flat regions where the local constraints having deficiency because of $|\nabla I| \approx 0$, the Horn-Schunck solution will use the regularizer $|\nabla u|^2 + |\nabla v|^2$ to fill in the flow information from neighboring fields. Therefore the Horn-Schunck method can effectively produce dense flow fields.

The combined local and global (CLG) method[10] introduces a new energy function which replaces the local constraint in the Horn-Schunck energy function E_{HS} with the Lucas-Kanade energy function E_{LK}

$$E_{CLG} = \int_\Omega (\begin{bmatrix} u & v & 1 \end{bmatrix} (G_\rho * \mathbf{J}) \begin{bmatrix} u \\ v \\ 1 \end{bmatrix} + \alpha(|\nabla u|^2 + |\nabla v|^2)) dxdy. \tag{16}$$

The solution $[u, v]^t$ that minimizes the E_{CLG} function satisfies the Euler-Lagrange equation

$$\triangle u - \frac{1}{\alpha}(G_\rho * (I_x^2 u + I_x I_y v + I_x I_t)) = 0, \tag{17}$$

$$\triangle v - \frac{1}{\alpha}(G_\rho * (I_x I_y u + I_y^2 v + I_y I_t)) = 0, \tag{18}$$

where $\triangle := \partial_{xx} + \partial_{yy}$.

The Euler-Lagrange equations can be solved iteratively through the successive overrelaxation (SOR) method. At each iteration, the flow estimates can be written as[4]

$$u_i^{k+1} = (1-\omega)u_i^k + \omega \frac{\sum_{j \in N_i^-} u_j^{k+1} + \sum_{j \in N_i^+} u_j^k - (h^2/\alpha)(J_{12i} v_i^k + J_{13i})}{|N_i| + (h^2/\alpha) J_{11i}} \tag{19}$$

$$v_i^{k+1} = (1-\omega)v_i^k + \omega \frac{\sum_{j \in N_i^-} v_j^{k+1} + \sum_{j \in N_i^+} v_j^k - (h^2/\alpha)(J_{21i} u_i^{k+1} + J_{23i})}{|N_i| + (h^2/\alpha) J_{22i}} \tag{20}$$

where i is the current point, N_i is the set of neighbor points of i, $N_i^- := \{j \in N_i | j < i\}$ and $N_i^+ := \{j \in N_i | j > i\}$, the superscript k indicates the iteration, and J_{nmi} is the (n, m)-th component of the structure tensor $G_\rho * \mathbf{J}$. $\omega \in (0, 2)$ is the relaxation parameter controlling the convergence. For $k = 0$, the initial values for the flow components are usually set to zeros, i.e. $u_i^0 = 0, v_i^0 = 0$.

3. JOINT EO AND IR OPTICAL FLOW ESTIMATION

Before optical flow estimation, the EO and IR images have to be carefully registered. The registration of images from different types of cameras is generally difficult, which involves the selection of features that are invariant across different cameras. The features can be contours or markers.[1] Registration is usually performed through perspective and affine transforms. The transform parameters are estimated based on the matched features. In a surveillance system, we may assume that the EO and IR cameras are mounted side-by-side and pointing to the same direction on a rigid structure, therefore the spatial and temporal constraints between the cameras are constants and known. Despite such setting, registration error may still occur because of parameter estimation error.

3.1. Motion from Color Method for EO and IR Images

We first investigate "motion from color" approach for joint EO and IR optical flow estimation. This is because infrared image can naturally be considered as an additional color component. According to brightness constancy assumption, we assume that the intensity value of a point in the IR image will not change under the motion of this point. The IR component provides an additional constraint. From equation (4) we have

$$\frac{\partial I_{EO}}{\partial x}u + \frac{\partial I_{EO}}{\partial y}v + \frac{\partial I_{EO}}{\partial t} = 0, \tag{21}$$

$$\frac{\partial I_{IR}}{\partial x}u + \frac{\partial I_{IR}}{\partial y}v + \frac{\partial I_{IR}}{\partial t} = 0, \tag{22}$$

where I_{EO} is the RGB intensity value, and I_{IR} is the IR intensity value of a point. I_{EO} can be calculated as

$$I_{EO} = 0.299 * I_R + 0.587 * I_G + 0.114 * I_B, \tag{23}$$

and we define

$$A = \begin{bmatrix} I_{EOx} & I_{EOy} \\ I_{IRx} & I_{IRy} \end{bmatrix}, b = \begin{bmatrix} -I_{EOt} \\ -I_{IRt} \end{bmatrix}. \tag{24}$$

We found that equations (21)-(22) produce more valid solutions than equations (5)-(7), because EO and IR constraints generally have less correlations than R, G, and B constraints. However the singular problem remains to be a major weakness of this approach. It is conceivable that in any flat region, partial derivatives over x and y in both EO and IR components will be close to zero, which creates a singular A^tA.

To overcome this problem, we use the condition number of A^tA to test its stability. If this number is larger than threshold, we explicitly set the flow estimation $\mathbf{u}$ to zero at this current point.

3.2. CLG Method for EO and IR Images

To adopt the CLG method for joint EO and IR optical flow estimation, we introduce two major modifications. First, we include a cross regularization mechanism in the CLG process for EO and IR images. Second, we devise a non-linear spatial flow fusion model which aligns the estimated motion fields from EO and IR images based on neighbor activities.

3.2.1. Cross-Regularization

We apply the CLG method separately to the EO and IR images. However during the iterative process, we introduce a cross-regularization mechanism which uses the current IR flow estimates to regularize EO estimation, and uses the current EO flow estimates to regularize IR estimation.

We first define a modified CLG energy function

$$E_{EO\_IR} = \int_\Omega (\begin{bmatrix} u_{M1} & v_{M1} & 1 \end{bmatrix} (G_\rho * \mathbf{J}) \begin{bmatrix} u_{M1} \\ v_{M1} \\ 1 \end{bmatrix} + \alpha(|\nabla u_{M1}|^2 + |\nabla v_{M1}|^2) + \beta(|\nabla u^-_{M2}|^2 + |\nabla v^-_{M2}|^2))dxdy. \tag{25}$$

where α and β are the regularization parameters, and $M1$, $M2$ indicate two modalities. If $M1$ is EO, then $M2$ is IR, and vice versa. $[u_{M1}, v_{M1}]^t$ are current flow estimates for either EO and IR images. $[u^-_{M2}, v^-_{M2}]^t$ are the flow estimates used in the cross-regularization terms. During the flow estimation for each particular image point i, $[u^-_{M2}, v^-_{M2}]^t$ represents a 2-D flow field obtained from $M2$ image except that the motion vector of the current point i is from $M1$ image. With this new energy function, the iterative equations in equations (19)-(20) become

$$u^{k+1}_{M1i} = (1-\omega)u^k_{M1i} + \omega \frac{\alpha \sum_{j\in N_i^-} u^{k+1}_{M1j} + \alpha \sum_{j\in N_i^+} u^k_{M1j} + \beta \sum_{j\in N_i^-} u^{k+1}_{M2j} + \beta \sum_{j\in N_i^+} u^k_{M2j} - h^2(J_{12i}v^k_{M1i} + J_{13i})}{(\alpha+\beta)|N_i| + h^2 J_{11i}} \quad (26)$$

$$v^{k+1}_{M1i} = (1-\omega)v^k_{M1i} + \omega \frac{\alpha \sum_{j\in N_i^-} v^{k+1}_{M1j} + \alpha \sum_{j\in N_i^+} v^k_{M1j} + \beta \sum_{j\in N_i^-} v^{k+1}_{M2j} + \beta \sum_{j\in N_i^+} v^k_{M2j} - h^2(J_{21i}u^{k+1}_{M1i} + J_{23i})}{(\alpha+\beta)|N_i| + h^2 J_{22i}}. \quad (27)$$

3.2.2. Flow Fusion Model

We also realize that cross-regularization alone can not provide the best solution. Each single modality may have missing information that can not be brought back by regularization. This calls for a spatial correlation model that can infer the missing information from the other modality. Towards this goal, we define a local activity measure and a non-linear rule that fuses the two estimated flow fields together.

Given the estimated flow fields $[u_{EO}, v_{EO}]^t$ and $[u_{IR}, v_{IR}]^t$, for each image point i, an activity measure is defined as

$$A_i = \sum_{j\in N_i} (u^2_{EOj} + v^2_{EOj})(u^2_{IRj} + v^2_{IRj}), \quad (28)$$

where N_i is the set of neighboring points of i. The flow estimate for point i can be decided based on a simple rule

$$u_i = \begin{cases} \max(u_{EOi}, u_{IRi}), & if A_i \geq Th_a \\ \min(u_{EOi}, u_{IRi}), & if A_i < Th_a \end{cases} \quad and\ v_i = \begin{cases} \max(v_{EOi}, v_{IRi}), & if A_i \geq Th_a \\ \min(v_{EOi}, v_{IRi}), & if A_i < Th_a \end{cases} \quad (29)$$

where Th_a is an activity threshold, and the max and min functions are based on magnitudes. This flow fusion method can be applied within the iterative flow estimation procedure or after the iterations are completed. However it is usually simpler to apply this at the end of the iterations.

4. EXPERIMENTAL RESULTS

We use the OTCBVS Dataset 03 "OSU Color-Thermal Database"[16] in the experiments. This dataset contains two surveillance type video sequences, each with an EO sequence and an IR sequence. Frame sizes are both 320×240. Sampling rates are approximately $30Hz$. EO and IR images are coarsely registered using homography with manually-selected points.

In the first experiment, we test the original "motion from color" method[8] and our modified method described in Section 3.1. The threshold on the condition number of the matrix A^tA is set at 20. All images are spatially smoothed using a 5×5 Gaussian filter with $\sigma = 2$. Flow estimation is based on the $10th$ frame, both in EO and IR, and the temporal derivatives are calculated from the $5th$ and the $15th$ frames. The results are shown in Figure (1). Because these are local methods, they can not produce dense flow fields. We can see that the results are generally noisy, and with many erroneous motions. However the joint EO/IR method clearly provides better motion fields, with less noisy motion and more accuracy around the moving object.

In the second experiment, we test our proposed joint EO/IR CLG method described in Section 3.2, and compare it with the original CLG method.[10] Flow estimation is based on the $5th$ frame, and the temporal derivatives are calculated from the $4th$ and the $6th$ frames. Image frames are temporally smoothed using a 5-tap Gaussian filter with $\sigma = 1.5$. The parameters in the CLG algorithm are: $\alpha = 10$, $\omega = 1.95$, $iteration = 50$. In the joint EO/IR CLG method, $\alpha = 8$ and $\beta = 2$. The activity threshold is $Th_a = 1$ in the first sequence, and becomes $Th_a = 20$ in the second sequence. Activity measure is calculated within a 5×5 neighbor set. The

results on the first sequence are shown in Figure (2) and the results on the second sequence are shown in Figure (3). From the results we can see that, in general the joint EO/IR CLG method produces better flow estimation than the CLG results from single modality. In the tests with the first sequence, the CLG performs better on the IR image than the EO image. This is partially because of strong sunlight and shadow effects in the EO image. In this case the joint EO/IR CLG method takes advantage of the IR component and produce even smoother motion filed. In the tests with the second sequence, The CLG performance is reversed, i.e. better on the EO image than the IR image. This is because the EO image scene is illuminated with diffused light, with very simple and clear background. In this case the joint EO/IR CLG method produces a flow field similar to the best of the CLG result. This is expected because the joint EO/IR CLG method is not to generate new information. It intends to improve the efficiency of information extraction from the same set of data.

5. CONCLUSION

In this work we studied optical flow estimation based on joint EO and IR image sequences. We investigated the "motion from color" method and the combined local-global method (CLG). During the modification of the CLG method for joint EO/IR processing, we introduced a cross-regularization mechanism and a non-linear flow fusion model based on local activity measures. Experimental results demonstrated the effectiveness of the proposed method. A possible future direction of our research is to develop fusion methods for multi-modal cameras from different view angles, which may provide more effective solution to 3-D flow field construction and occlusion elimination.

REFERENCES

1. J. Kang, K. Gajera, I. Cohen, and G. Medioni, "Detection and tracking of moving objects from overlapping eo and ir sensors," in *the Joint IEEE International Workshop on Object Tracking and Classification Beyond the Visible Spectrum*, pp. 123–128, (Washington, DC), 2004.
2. J. Kang, I. Cohen, and G. Medioni, "Persistent objects tracking across multiple non overlapping cameras," in *the IEEE Workshop on Motion and Video Computing (WACV/MOTION05)*, **2**, pp. 112–119, (Washington, DC), 2005.
3. B. Horn and B. Schunck, "Determining optical flow," *Artificial Intelligence* **17**, pp. 185–203, 1981.
4. A. Bruhn, J. Weickert, and C. Schnorr, "Lucas/kanade meets horn/schunck: Combining local and global optic flow methods," *International Journal of Computer Vision* **61(3)**, pp. 211–231, 2005.
5. B. Lucas and T. Kanade, "An iterative image registration technique with an application to stereo vision," in *Seventh International Joint Conference on Artificial Intelligence*, pp. 674–679, (Vancouver, Canada), 1981.
6. B. Lucas, *Generalized image matching by the method of differences*. PhD thesis, School of Computer Science, CarnegieMellon University, Pittsburgh, PA, 1984.
7. J. Bigun and G. H. Granlund, "Optical flow based on the inertia matrix in the frequency domain," in *SSAB Symposium on Picture Processing*, (Lund, Sweden), 1988.
8. P. Golland and A. M. Bruckstein, "Motion from color," *Computer Vision and Image Understanding* **68(3)**, pp. 346–362, 1997.
9. H.-H. Nagel, "Constraints for the estimation of displacement vector fields from image sequences," in *Eighth International Joint Conference on Artificial Intelligence*, **2**, pp. 945–951, (Karlsruhe, West Germany), 1983.
10. A. Bruhn, J. Weickert, and C. Schnorr, "Combining the advantages of local and global optic flow methods," *Pattern Recognition* **2449**, pp. 454–462, 2002.
11. T. Brox, A. Bruhn, N. Papenberg, and J. Weickert, "High accuracy optical flow estimation based on a theory for warping," in *Eighth European Conference on Computer Vision*, **4**, pp. 25–36, (Prague, Czech Republic), 2004.
12. J. L. Barron, D. J. Fleet, and S. S. Beauchemin, "Performance of optical flow techniques," *International Journal of Computer Vision* **12(1)**, pp. 43–77, 1994.
13. H. W. Haussecker and D. J. Fleet, "Computing optical flow with physical models of brightness variation," *IEEE Trans. on Pattern Analysis and Machine Intelligence* **23(6)**, pp. 661–673, 2001.

14. M. Bertero, T. A. Poggio, and V. Torre, "Ill-posed problems in early vision," *Proceedings of the IEEE* **76(8)**, pp. 869–889, 1988.
15. N. Ohta, "Optical flow detection by color images," in *IEEE International Conference on Image Processing*, pp. 801–805, (Singapore), 1989.
16. "http://www.cse.ohio-state.edu/otcbvs-bench/."

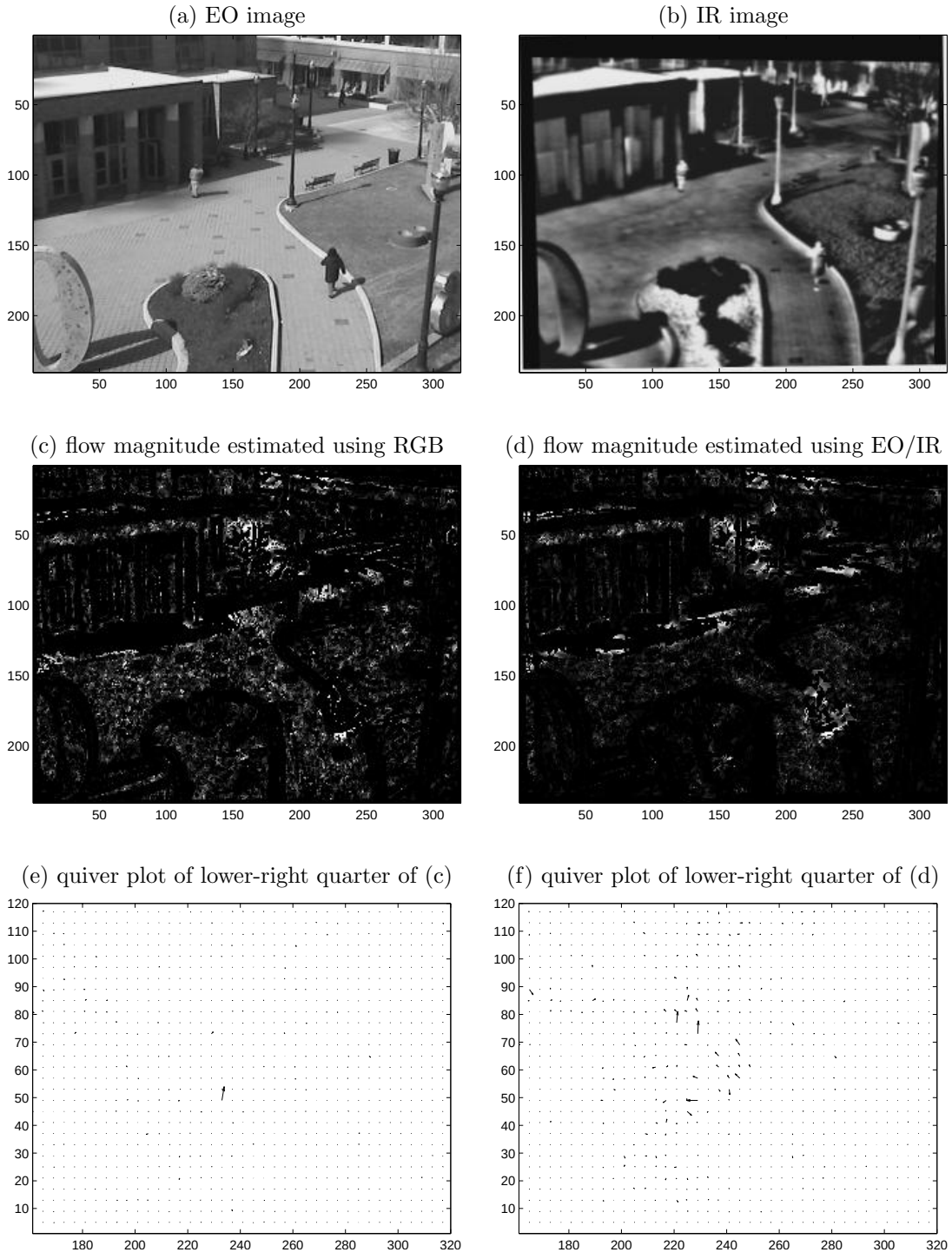

Figure 1. Optical flow estimation using "motion from color" methods on the first sequence.

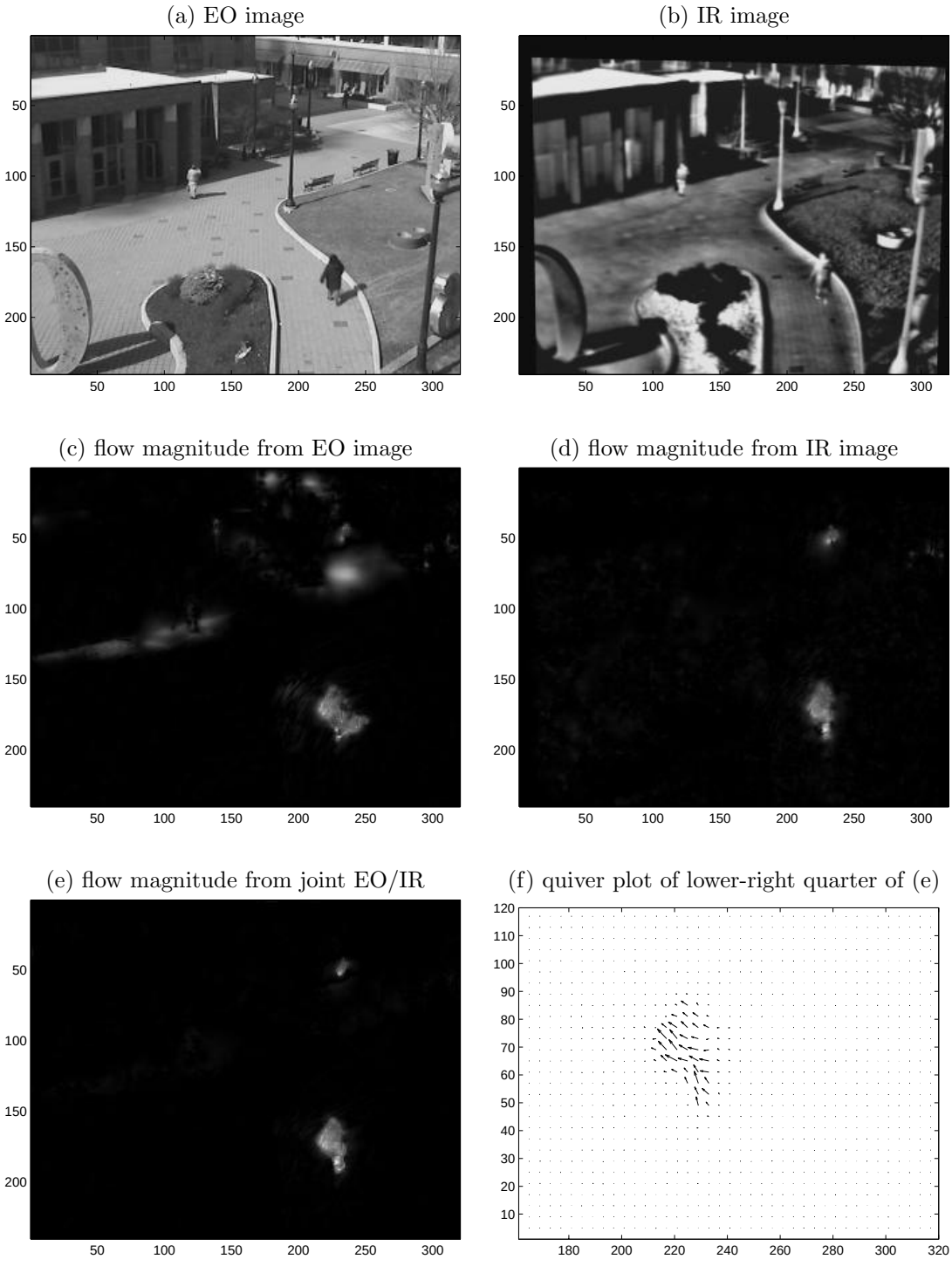

Figure 2. Optical flow estimation using CLG and joint EO/IR CLG methods on the first sequence.

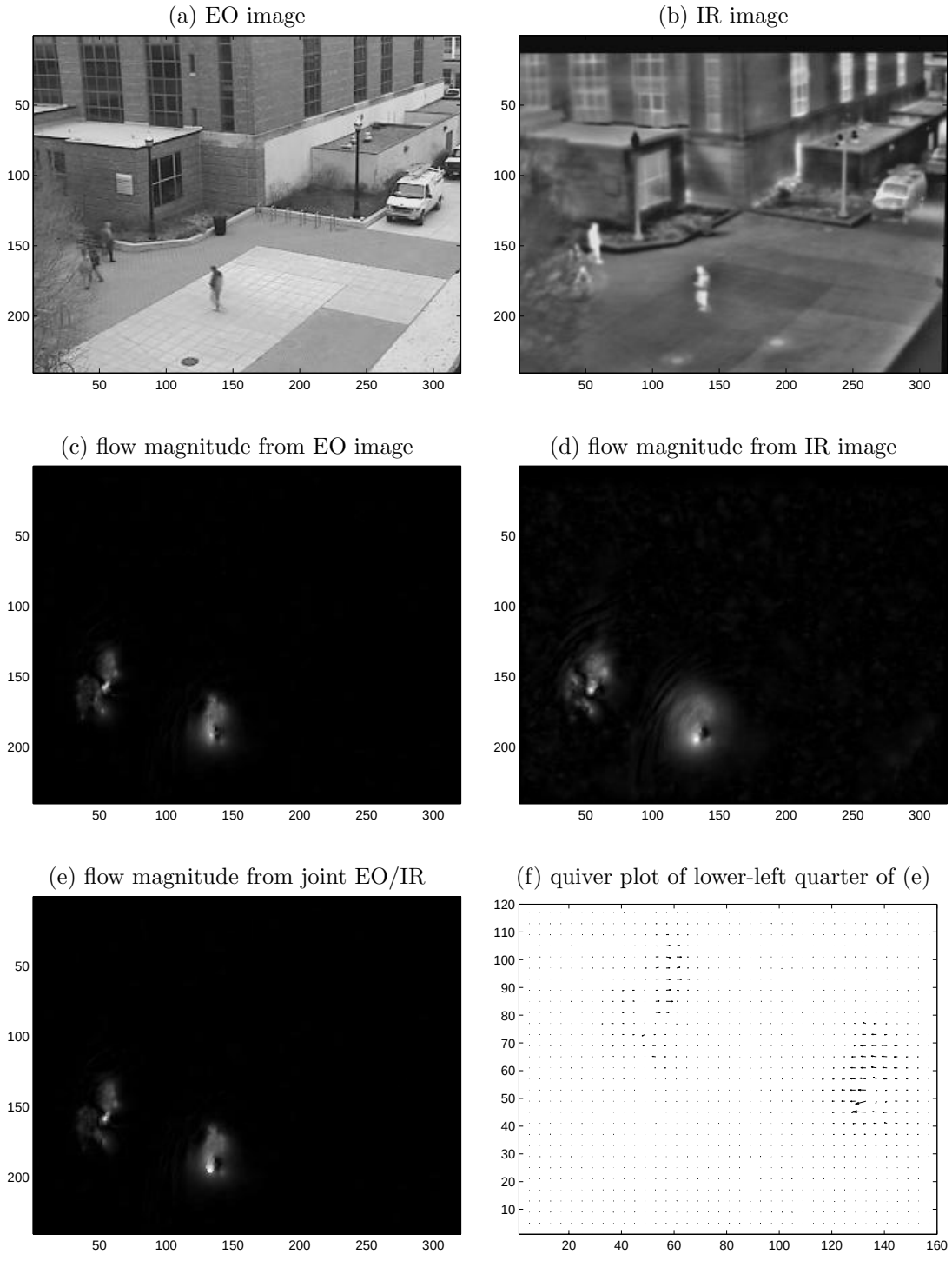

Figure 3. Optical flow estimation using CLG and joint EO/IR CLG methods on the second sequence.